Sustainable Materials and Technologies 42 (2024) e01174

Contents lists available at ScienceDirect

Sustainable Materials and Technologies

journal homepage: www.elsevier.com/locate/susmat

Separation of adhesive joints of pouch cells in the context of battery module disassembly

Dominik Goes *, Eduard Gerlitz, Matthias Kagon, Hendrik Möllers, Florian Kößler, Jürgen Fleischer

wbk Institute of Production Science, KIT Karlsruhe Institute of Technology, Kaiserstraße 12, 76131 Karlsruhe, Germany

ARTICLE INFO

Keywords:
Disassembly
Adhesive joints
Battery

ABSTRACT

The increase in demand for electric vehicles due to the transformation to electromobility will lead to a large number of batteries reaching the end of life and needing to be disposed of. Direct recycling of batteries requires disassembly down to cell level. However, adhesive bonds present a major obstacle to mechanical disassembly. In this work, adhesive bonds between pouch cells are characterised and possible separation processes are identified. Based on this, an industrial system concept for cutting the adhesive bonds, particularly with a rope cut, is developed and tested. A stable and safe process parameter space was identified. The separation process can enable further circular economy strategies such as remanufacturing or reusing the battery cells.

1. Introduction

1.1. Motivation

Over the next decade, demand for electric cars is expected to grow rapidly. This will initially lead to an increase in demand for raw materials for battery production and, in the long term, to a large quantity of old batteries that will have to be disposed of [14]. At the end of a lithium-ion battery's life cycle, the question of optimal disposal arises. Traditional methods such as landfill or incineration for energy recovery are unsuitable. Landfill pollutes the soil and groundwater over time. Incineration produces toxic gases. In addition, valuable metals such as lithium cannot be recovered using these methods. They would have to be mined again to manufacture new batteries, resulting in major pollutant emissions and financial costs. It is therefore important to recycle old batteries and reuse the recovered raw materials to produce new batteries. This reduces the environmental impact of battery production and lowers the cost of battery production [7,16,25].

Current state of the art recycling processes, such as pyrometallurgical recycling, which melts down complete battery modules, only partially meet the requirements for an ideal recycling process. They are often energy and cost intensive [34]. As a result, they lead neither to a better environmental balance nor to a reduction in manufacturing costs [7]. Newly developed recycling processes, such as direct recycling, promise an improvement here. On a laboratory scale, these techniques can recover a large proportion of the raw materials used in the battery. In these processes, the battery cannot be processed as a whole, but must be separated into its individual fractions as far as possible. Currently, this disassembly is not yet economically feasible on an industrial scale [27]. Adhesive bonds are a major barrier to battery module disassembly. They are not designed to be detached and are often located in hard to reach areas of the battery module. Current separation processes are mainly manual and are therefore time consuming and costly. In addition, the composition of the battery poses a health risk to the worker performing the separation [21,24].

To increase the cost-effectiveness of these newly developed processes, an automatic or semi-automatic disassembly process for battery modules and the adhesive joints used in them needs to be developed.

Direct recycling requires disassembly down to cell level. At the same time, more granular disassembly opens up new possibilities with regard to alternative circular economy strategies, such as reuse or repurposing [21].

Many types of adhesive are used in battery modules. The exact amount and location within the battery module depends on the function of the adhesive. For example, in Li-ion pouch cell modules, the individual battery cells are often glued together to ensure optimum thermal contact from cell to cell [5,24]. The adhesives used are usually epoxy, acrylate, polyurethane or silicone based [30].

The design of a battery system places special demands on the thermal management. Heat is generated during operation, charging and braking

* Corresponding author.
E-mail address: dominik.goes@kit.edu (D. Goes).

https://doi.org/10.1016/j.susmat.2024.e01174
Received 26 April 2024; Received in revised form 10 August 2024; Accepted 27 October 2024
Available online 10 November 2024

(recuperation). Heat can be supplied and dissipated in a number of ways. Thermally conductive adhesives and thermal interface materials are a proven solution. Adhesives are also gap-filling and resistant to most process fluids. They are also used to compensate for manufacturing tolerances. Their main application in battery modules is to bond the battery cells and the cooling system [2,4,28,30]. Other adhesives used in battery modules which are not looked at in this paper are:

- Encapsulants used as coatings to protect sensitive parts from dust and moisture
- Threadlocker adhesives to secure screws
- Sealants to protect the battery cells from environmental influences
- Electrical adhesives for connecting cells

There are several methods of classifying adhesives. The two most common are classification by chemical type and curing mode. There are two chemical types of adhesives: organic and inorganic with silicones as a third group with characteristics of both types. Organic adhesives are further divided into natural adhesives (e.g. starch) and synthetic adhesives (e.g. epoxy). For industrial use, synthetic adhesives are usually more suitable due to their higher bond strength. The two main types of curing are chemical and physical curing. Chemical curing involves the reaction of two components to form a polymer, often resulting in high bond strength. All adhesives used in this paper cure chemically [19,20].

The adhesives considered in this paper are structural adhesives. Structural adhesives have a high strength, which increases the disassembly effort compared to other adhesives. Structural adhesives are used to hold cells in place. They are either strategically placed between cells or between cells and housing parts. In pouch cells structural adhesives with increased thermal conductivity can be used to improve heat flow to and from the cell. Adhesive tapes are often used as an alternative to liquid adhesives, as they are easier to handle during manufacturing [3,4,22]. This paper focuses on the adhesive joint between the cells, since damage to the cells during disassembly has the most serious consequences. In addition, only the joint between pouch cells is considered, as the thin pouch foil is most susceptible to damage during disassembly.

The adhesive joints between two pouch cells can be seen in the example of the separated cells from a Nissan Leaf battery module in Fig. 1.

When operating in an electric vehicle, pouch cells must be able to withstand external influences such as thermal and mechanical stress. These requirements must also be taken into account when developing a safe disassembly process. In contrast to lithium-ion cells with a hard casing, pouch cells are much more sensitive to temperature [18]. According to the DIN EN 62660–3 test standard, Li-ion cells must withstand a temperature change from RT to a maximum of 65°C within 90 min at 80 % state of charge. The maximum temperature limit according to the test standard are 130°C (100 % state of charge) [10]. Mechanical stress, such as bending, can lead to cracking of the electrode tabs and external short circuits, which can be catastrophic [23]. Keshavarzi et al. investigated the mechanical properties of pouch cells. Between 317 N and 430 N force, a deformation of the cell was observed in three-point bending tests. Qu et al. demonstrated a displacement of 1 mm at a force of 50-100 N in an experimental three-point bending test on a commercial pouch cell, and a displacement of 2 mm at a force of 50-160 N [31]. The studies demonstrate the vulnerability of pouch cells to deformation even at low forces. Although sealed pouch cells provide a lightweight solution to the battery pack, they are more susceptible to certain types of damage than cells enclosed in rigid metal cases. The overall aim is to ensure the process-safe separation of adhesive joints in the context of the industrial disassembly of Li-ion traction batteries. The focus of the following investigation is on the glued connection between two pouch cells as it is the most critical joint.

The aim of this paper is to identify and characterise the most suitable separation process. As already mentioned, the focus is limited to mechanical processes. At the same time, an industrially applicable system for the process is to be designed and tested in principle. In a the first step, a systematic comparison of alternatives and a pre-selection of suitable separation processes according to Fig. 2 will be carried out. The preselection here is peeling, shearing, rope cutting. In the next step, the peeling and shearing processes will be characterised in principle, especially with regard to the material-adhesive pairing and evaluated in preliminary investigations. Peeling and shearing will be investigated as suitable methods for the separation of adhesive bonds between the two cells and, in particular, an influence quantity analysis will be carried out. In the third step, process qualification and characterisation will be carried out for rope cutting as another promising process. Firstly, the basic suitability will be demonstrated through qualification tests. This will be followed by an analysis of the various influencing factors. From this, a comparability or transferability to peeling and shearing will be concluded. An important focus of the influence factor analysis will be on the defect patterns of the separation samples, such as surface damage or plastic deformation of the pouch foil, resulting from the process instability. The final step will be to develop an industrial plant concept for cutting the bonded joint based on the results of the tests, in particular with rope cutting. This will be tested in principle.

1.2. State of the art

According to DIN 8591 [13], the separation of adhesive joints is part of the disassembly of components or assemblies. It is the"disassembly of parts joined by adhesive bonding (see DIN 8593–8) [12] by overcoming the adhesive force, provided this can be done without damaging the joined parts".

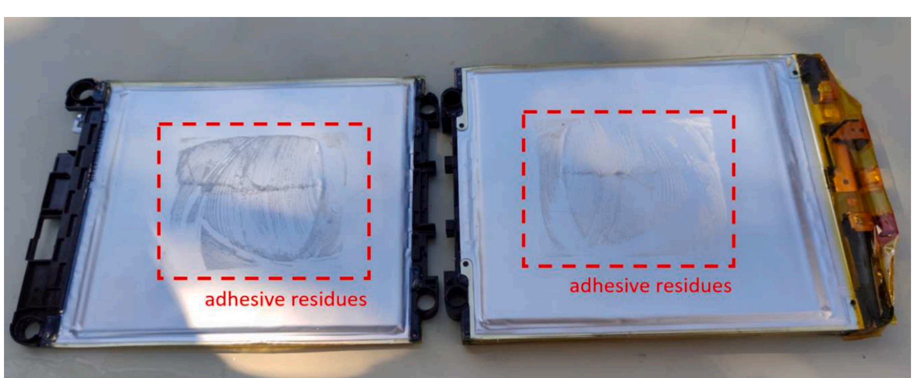

Fig. 1. Adhesive residue on two separate battery cells of a Nissan Leaf battery module. A Nissan Leaf battery pack is made up of several battery modules. Each battery module is made up of four battery cells, which are stacked and glued together. Each battery cell is in the form of a pouch cell. The two pouch cells shown in the illustration have been disassembled by hand by separating them at the marked adhesive areas. The dimensions of a pouch cell are approximately 300x200mm.

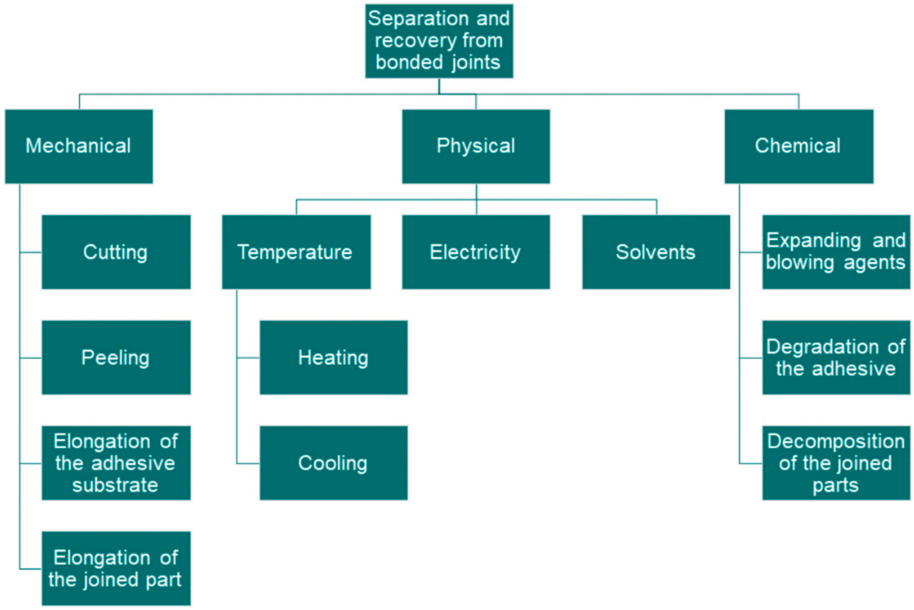

Fig. 2. Systematics of the main and subgroups for separating and recovering joined parts and adhesives from bonded joints [8].

DIN/TS 54405 [8] identifies and describes some common methods for the separation and recovery of adhesives and bonded parts from bonded component joints. Separation can be divided into three mechanisms, physical, chemical and mechanical. However not every possible mechanism is suitable for every bond.

Chemical methods of reducing bond strength include the use of solvents and other reactive substances that cause partial dissolution or decomposition of the adhesive [33]. In the case of chemical methods, decomposition of the bonded parts to be joined cannot be ruled out as there is no targeted separation. Access to the joint between two cells is also limited and the penetration of a solvent can be very time consuming. The use of solvents is therefore not recommended.

Debonding by heat or freezing is a physical process. In thermal debonding, the joint is heated and the strength of the adhesive is significantly reduced so that the parts can be separated by applying a small amount of force. The glass transition temperature of the adhesive is exceeded. Conversely, if elastomers are used above the glass transition temperature, the glass transition temperature is lowered to achieve embrittlement of the adhesive. However, there are limits to the usable temperature and exposure time imposed by the battery cell. These must be respected. The physical processes can be used as an aid for separating battery cells if the temperature limits are observed. If the adhesive force is too great to be overcome directly by mechanical methods, it is necessary to reduce it by thermal methods. Heating of the adhesive can reduce the bond strength. Alternatively, cooling of the bond can cause the adhesive to become brittle, reducing the bond strength. The use of high or low temperatures can therefore reduce the bond strength and thus reduce the process forces in mechanical processes [1,6].

In their work, Kovachev et al. analyse Li-ion cells by generating microscopic images. To gain access to the cells, they use a 0.7 mm diameter nylon rope to manually separate the glued cells after spraying the bonded areas with solvent. The exposure time is 3 min [24]. Solventing particularly thin bonds can take a long time as the solvent penetrates slowly [32]. A similar process takes place when windscreens are removed from a vehicle. Lammel and Schaumeier report two different processes using wire and an oscillating blade. Both processes are performed manually. An oscillating blade often causes damage to the joining part [26]. In addition, the separation of adhesive-bonded Li-ion cells has not yet been considered in the literature.

The state of the art of separation processes for joints similar to bonded battery cells shows that mechanical separation processes can be suitable solutions for the separation of pouch cells. This paper will therefore focus on mechanical processes. Physical processes such as the application of temperature as an aid to disassembly (to reduce separation forces) are being analysed. However, not every possible mechanical method is sufficient, as damage to the battery cells must be avoided at all costs. Cutting and peeling should be analysed according to DIN/TS 54405 (Fig. 2). In addition to peel stress, bonded joints may also be subject to shear stress. Therefore, shearing should also be analysed. After the derivation of these three methods, they are presented and analysed in more detail in the following chapter.

2. Materials and methods

A distinction is made between pre-testing, where the peeling, shearing and wire cutting processes are analysed, and industrial testing, where an industrial prototype machine is developed to represent the cutting process.

2.1. Pre-tests

To investigate the peeling, shearing and wire cutting processes, commercially available pouch foils were glued with common adhesives and then tested to replicate reality. The pouch foil is a laminate of aluminium and two polymers. The aluminium (approx. 40 μm) is coated on one side with a layer of polyamide (PA) (approx. 40 μm) and on the other side with a layer of polyethylene terephthalate (PET) (approx. 80 μm). The types of adhesives used to bond the pouch foil together are shown in Table 1. In preparation for the bonding process, the pouch foil was cut into sheets according to the standard testing procedure used (DIN EN ISO 11339:2010–06 for T-peel test and DIN EN 1465:2009–07 for Tensile shear strength). To improve adhesion, the polyamide surface representing the outer layer of the pouch cell was cleaned with isopropyl

Table 1
Overview over used adhesives.

Base	Components
Epoxy 1 (EA9497)	2
Polyurethane 1 (7800 A/CD)	2
Acryle	2
Acryle	Tape

alcohol and lint-free wipes. After drying, the adhesives were applied. In the case of the two-component adhesives, a static mixing nozzle was used to mix the adhesive homogeneously. For the full-surface bonds for the peel and wire cut tests, the two-component adhesive was applied to the foil in a meandering pattern. The tape was used to position the strips flush against each other. After the adhesives were applied, the second pouch foil was placed and the bond was pressed between the sheets with weights to achieve a uniform distribution and wetting of the adhesives in the bond. Curing was carried out at room temperature with regular humidity. After the recommended curing time, the sheets were cut to the required specimen shape using a lever cutter.

A tensile testing machine from ZwickRoell (Zwicki RetroLine 2.5 kN) was used as the test rig for the measurements to investigate the peeling and shearing processes. It was fitted with an Xforce P 2.5 kN load cell with a nominal maximum force of 2.5 kN. The recording and pre-evaluation of the measurement according to the test standard was carried out in the TestXpert 3 sofware. The measured values obtained were also exported and fitted to be evaluated with the use of Matlab scripts and MS Excel.

Shear and T-peel tests were performed to characterise the adhesion of each adhesive to the pouch foil and confirm their suitability for further testing. The shear tests were performed according to DIN EN 1465:2009–07 [11]. Two 100 mm* 25 mm pieces of foil were glued together with a bond area of 12,5 mm*25 mm. T-peel tests were performed according to DIN EN ISO 11339:2010–06 [9]. 250 mm*25 mm samples were made with a bond area of 200 mm*25 mm. The samples were tested using the standard jaws supplied with the test rig.

In order to investigate the separation of the pouch foil samples by wire cutting, a custom built wire cutter was developed and installed on the described test rig. The test setup and wire clamping mechanism is shown in Fig. 3. The lower clamp forms a U-shape in which a wire is mounted. Two stacked strips of pouch foil are clamped in a lateral force-fit at the upper clamping unit. The wire of the lower clamping unit (U-shape) is located between the two strips of pouch foil. Both strips are glued together underneath the wire. By moving the upper clamping unit upwards, these strips are also moved upwards. The wire in between separates the strips from each other by wire cutting at the adhesive area. The load cell of the test rig measures the force required to separate the glued strips by wire cutting. The U-shaped frame shows high rigidity against mechanical forces. However, when forces above 200 N were applied, it showed visible elastic deformation. This is caused by the 3D-printed beam which is made of PET-G to provide electric insulation. In order to investigate several influencing factors, such as the wire temperature, an electrical heating and wire temperature measurement is included in the setup. The wire temperature is measured using a NTC resistor. Due to the small diameter of the wire, the NTC chosen has a similar size to reduce the influence of the environment. The temperature was set up prior to the tests as the wire cooled down rapidly once in contact with the specimen, while the wire outside the sample remained hot. It was not possible to place the resistor in the occurring joint gap as in some cases the wire twisted under the influence of the forces. Prior to the test, the wire was preheated for 15–30 s to reach the test temperature. As there are no comparable and known standard test procedures, the specimen geometry was selected based on DIN EN ISO 11339 [9].

Given the setup, wire geometry, wire temperature and cutting speed were investigated as these factors promised the greatest influence on the required cutting force. These four factors were combined according to Design of Experiments (DoE) practices. To statistically validate the results, each combination of parameters was tested five times resulting in a total of approximately 330 measurements. The measured values obtained in this way were adjusted by an outlier test [15] and fed into the analysis of variance [29].

2.2. Industrial tests

Dummy pouch cells were produced to investigate the wire cutting process. The same pouch foils as described above were used for the dummy cells. The pouch foils were cut with a lever cutter to common sizes used for traction batteries in electric mobility. A size of 235 mm* 180 mm was used for the pouch foils, including the sealing edge (≈ 10 mm per edge). The pre-cut pouch foils were deep-drawn using a deep drawing-press with a punch size of 222 mm* 168 mm (Fig. 4a). The press

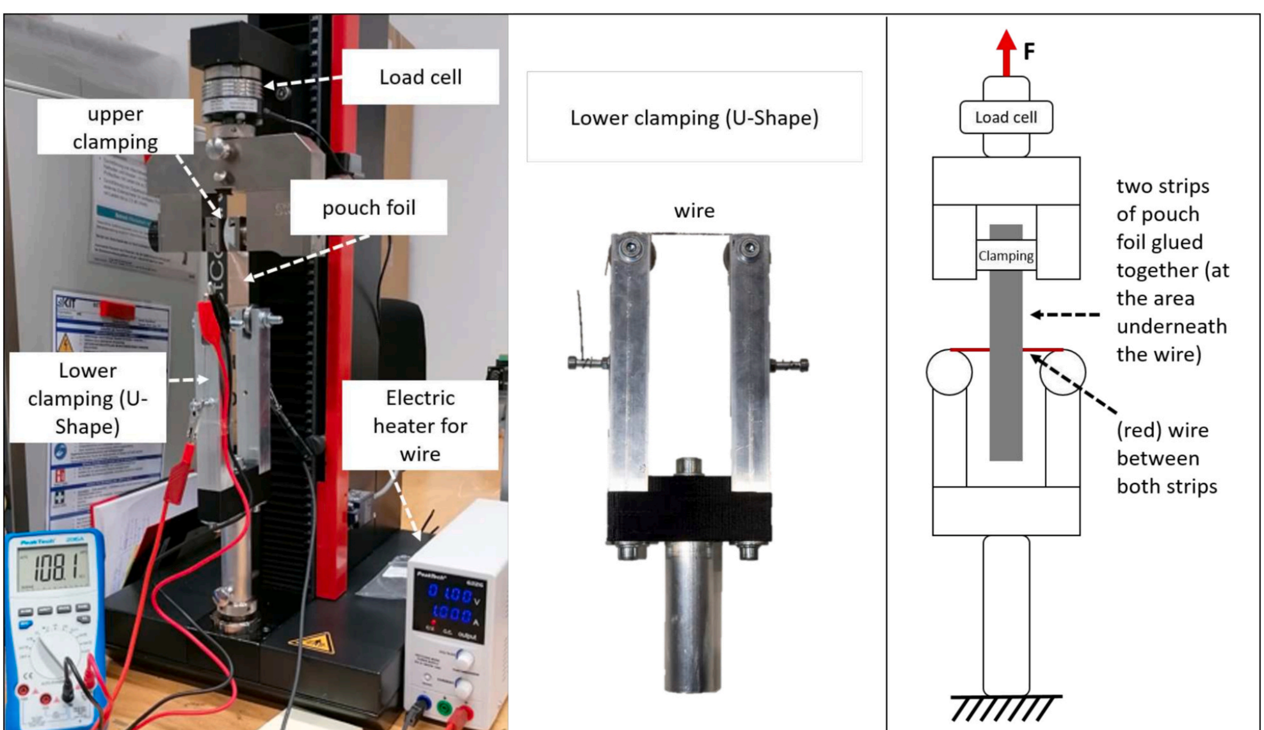

Fig. 3. Test setup for characterising the adhesive force and process force during wire cutting. The wire can be heated using electric heating.

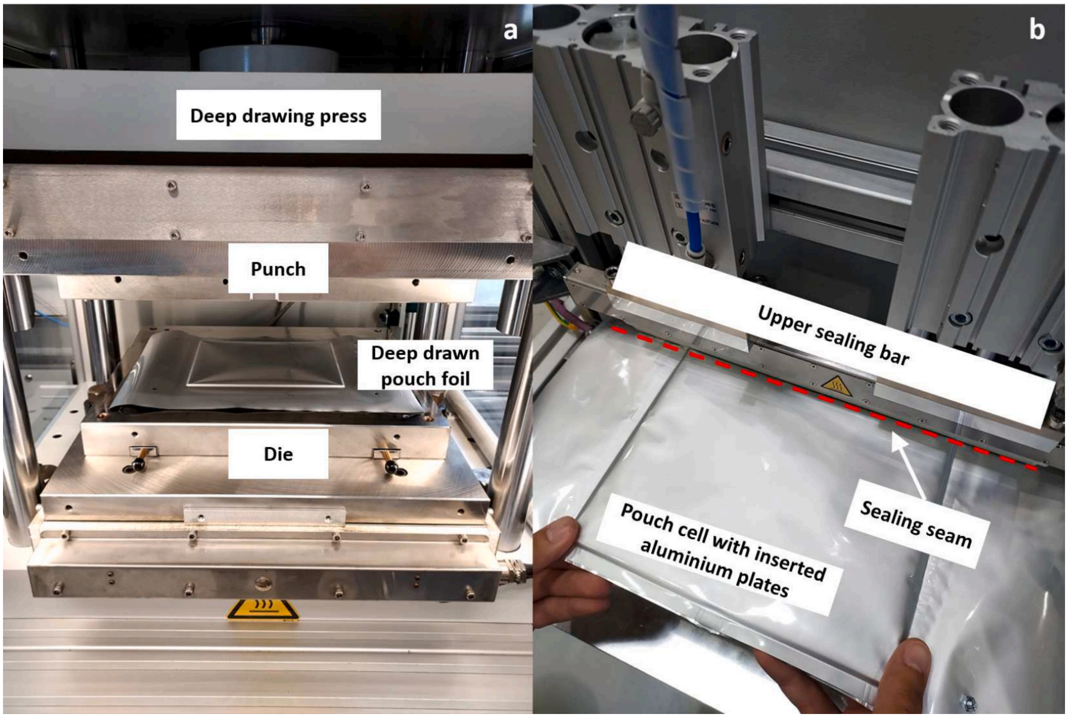

Fig. 4. Preparation of the pouch cells: deep drawing (a) and sealing (b).

force ≡ 60kN and deep drawing depth ≡ 4 mm were selected for the deep drawing process. Aluminium plates were inserted into the deep-drawn half-shell pouch foils to mimic the cell components anode, separator, cathode and electrolyte. The dummy cells were evacuated by pressing weights on both sides and then sealed airtight using sealing bars (Fig. 4b). The sealing seam is highlighted in Fig. 4b) with a dotted red line. To bond two dummy cells together, three 160 mm* 25 mm strips of 3 M adhesive tape (3 M GPH-060GF) were applied in parallel to an outer cell surface (Fig. 5a). This adhesive tape allows a specific gap between two cells and was therefore chosen for the tests. To investigate the separation process, two bonded pouch cells were placed in the vacuum clamping system of the industrial cell separator. A gap of 2-3 mm is created between the glued cells. The upper cell was controlled and clamped from above by a kinematic with a suction pad. A loop wire from Diamond WireTec GmbH & Co.KG (Diamond Wire Loop, length 2 m, diameter 0.6 mm, tensile strength 120 N; DWL.MS-060D-D91–2000 L) was fixed and tensioned on the driven wheel unit. In Fig. 5b the loop wire is highlighted with a red dotted line. The workpiece (pouch cells) and tool (loop wire) are positioned by moving the lift table vertically to the correct height and then moving the synchronized traversing axes horizontally (Fig. 5b).

3. Results and discussion

3.1. Qualification and characterisation of the separation process in pre-tests

In the course of research into suitable separation processes for adhesive bonds in battery modules, DIN/TS 54405 [8] provided a guideline of known processes for breaking the material bond through the adhesive. According to DIN/TS 54405 [8], the separation processes can be divided into 3 basic mechanisms”mechanical”,”physical”

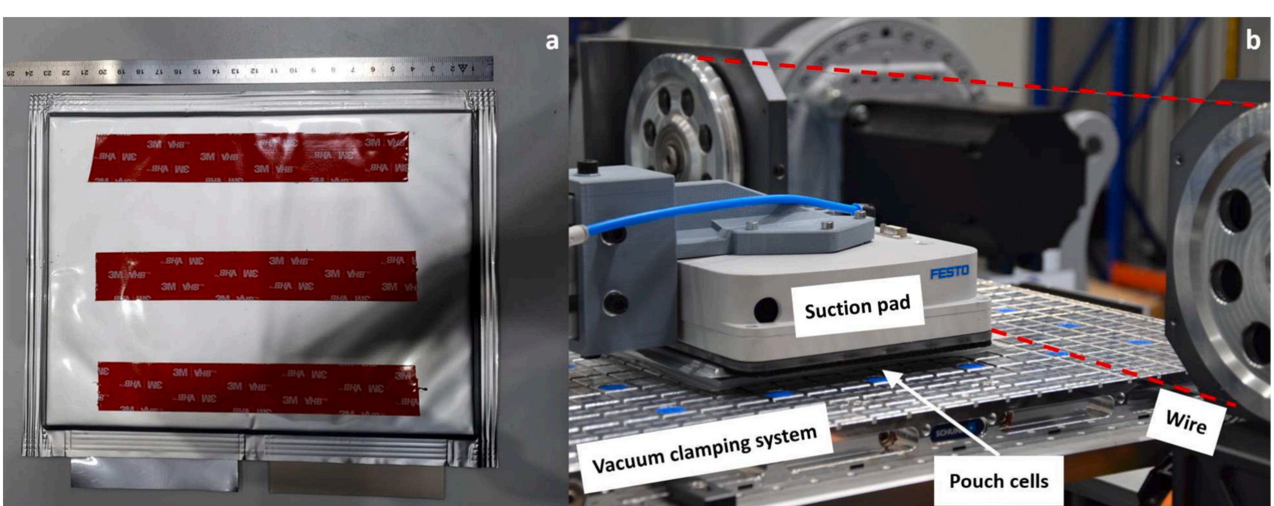

Fig. 5. Gluing the pouch cells (a) and preparing of the separation system (b).

and"chemical" (see Fig. 2). However, taking into account the framework conditions provided by the modules, most of the processes are eliminated. This is because certain processes do not appear to be suitable from an economic and safety point of view, because the expected process times are too long, or because other separation processes have a damaging effects on the cells, such as the elongation of the joining parts or decomposition of the joining parts. This leaves 'shearing', 'peeling' and 'cutting' from the group of mechanical processes, and 'heating' as a physical process. These processes are selected and characterised for the pre-tests. Heating is limited by the cell, as otherwise a thermal runaway can occur, which must be avoided at all costs.

The results of the qualification and characterisation of the pre-selected processes are presented below. The analysis is based on the force curve, which is an indication of the process stability. The maximum force during separation is used as a comparative measure, which is important for the design of industrial equipment, among other things. The fracture patterns are also analysed, providing information on the fracture mechanism. The results of the significance analysis of the influencing factors using rope cutting are also presented.

3.1.1. Cutting force

The maximum forces during separation are shown in Fig. 6. The shearing is abrupt and not gradual as in peeling and rope cutting. Very different forces are observed for the same separation process and different adhesives. It has not been possible to establish principles for the same adhesive and different methods of separation. Adhesive bonds seem to behave differently in different load cases (shear vs. peel). Polyurethane showed the highest shear and rope cut forces, while acrylic tape showed the highest T-peel force. Not only the force required but also the standard deviation during rope cutting was highest for polyurethane, which may indicate an unstable process. The large deviation is due to the adhesive and not to the process, as it only occurred with polyurethane. The lowest forces were always measured during T-peeling. The highest forces generally occurred during shearing. Shearing has a peculiarity compared to peeling and rope cutting. Whereas in peeling and rope cutting the force is only dependent on the width of the bond, in shearing the depth of the bond is an influencing factor. For example, shear forces can be very high if the bond is deep, whereas peeling and rope cutting forces are limited. Rope cutting and T-peeling are therefore particularly suitable for cutting forces, depending on the adhesive.

3.1.2. Fracture patterns

An overview of the fracture types for the three different tests with the four adhesives is summarised in Table 2. A distinction is made between Adhesion (A) and Cohesion fracture (K). Adhesive fracture means that the adhesive forces (force between adhesive and substrate) are less than the cohesive forces (internal forces within the adhesive). This fracture pattern indicates inadequate adhesive adhesion to the joining part, for example, due to improper surface preparation or adhesive selection. The reverse is true for cohesive fracture. This fracture pattern indicates poor stability of the cured adhesive for example due to internal weaknesses or insufficient adhesive strength. In the case of a combined fracture, both types of force are similar. In particular, this shows that adhesion fractures (A) predominantes. Adhesive fractures with a small proportion of cohesive fractures (K) were observed when adhesive bonds were separated using adhesive tape. When polyurethane samples were separated by rope cutting, a combined adhesion and cohesion fracture occurred. Plastic deformation occurred in all shear tests. The highest forces were also measured during shear. Shearing the polyurethane samples tore the pouch foil. In this case, the tensile strength of the foil is less than the adhesive strength of the adhesive. This would lead to damage to the battery cell in a separation test with real pouch cells and must be avoided. This result indicates that shearing is not suitable as a separation process due to damage.

3.1.3. Influencing factors

Based on the statistical evaluation, it was also possible to identify influencing factors that have a statistically significant effect on the target value of the cutting force. Within the samples of the same

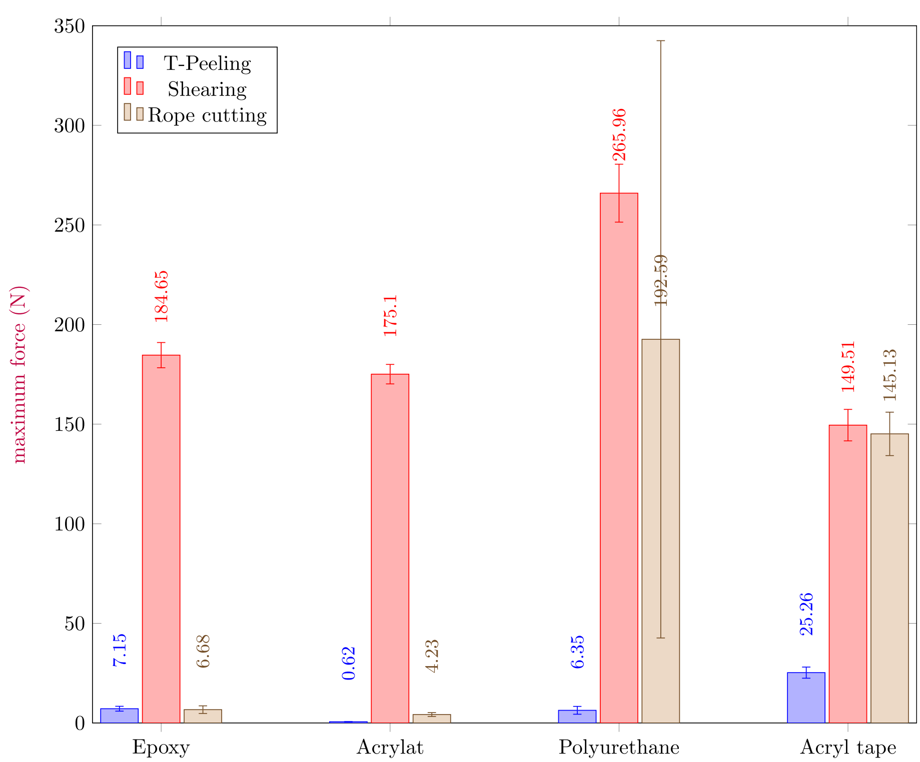

Fig. 6. Maximum forces for various disassembly methods and different types of adhesive.

Table 2
Fracture patterns and plastic deformations for different adhesive bonds and separation methods.

	Epoxy	Acrylate	Polyurethane	Acrylic foam (Adhesive tape)
	Henkel Loctite EA 9794	LORD 850/25GB	LORD 7800/A/D	3 M GPH-060GF
Fracture pattern				
T-Peeling	A	A	A	A (small portion K)
Shearing	A	A	–	A
Rope cutting	A	A	A/K	A (small portion K)
Plastic deformation				
T-Peeling	–	–	–	–
Shearing	x	x	X (Cracked)	x
Rope cutting	–	–	X	x

adhesive, it was found that the cutting wire temperature as well as the cutting speed and the cutting wire geometry were found to have a statistically demonstrable influence on the system.

By heating the wire, a change in the fracture pattern from adhesive fracture to cohesive fracture could be achieved, especially at low cutting speeds. This significantly reduced the cutting force required. In addition, the scatter and the oscillation amplitude of the cutting force were significantly reduced. This effect could not be maintained at high cutting speeds, so that a cohesive fracture often prevailed in the early part of the cut (due to the preheating time of the wire), which changed to an adhesive fracture in the further course of the measurement. The reason for this is probably that the heat was applied to the bond for too short a time to achieve softening or melting.

Evaluation of the individual measurements using ANOVA shows that no general parameterisation of the process is possible. Rather, it was shown that the optimal parameters depend on the adhesive as well as on the target value considered (maximum force). Regarding the cutting forces, it can be generalised that lower cutting speeds correlate with lower cutting forces. Especially with the adhesive tape using wire heating, the cutting forces could be reduced by a good 50 %. On the other hand, reduced cutting speeds increase the required process time and in combination with a heated wire, increase the risk of thermal damage to the cell. In the case of the epoxy adhesives, however, the heating of the wire causes a slight increase in the cutting force, as post-curing can occur due to the heat input. A significant influence of the wire geometry was also found in some cases. In the case of epoxy resin, the lowest median forces were found with the round wire, for example, while in the case of acrylic tape the lowest median forces were found with the twisted wire. The results of the ANOVA are summarised in Table 3.

3.1.4. Summary and conclusion

Since deformation of the pouch foil occurred with each shearing and the highest forces were also observed, shear can be ruled out for the separation of glued pouch foils. According to Gerlitz et al., the greatest danger is the destruction of the unstable cell housing of pouch cells and the associated leakage of the electrolyte [17]. A major weak point can be the sealed seam, which can be torn open by high forces. During peeling, the lowest peel forces were achieved with all the adhesives used and no deformation of the pouch foil occurred. From this point of view, peeling appears to be the most suitable release method. Nevertheless, due to the required high deformations required for the entire lithium-ion cell, peeling does not appear to be suitable for separation adhesive bonds within battery modules. The deformations can cause damage to the separator and electrodes of the individual cell, which according to Gerlitz et al. represents a significant safety mechanical risk [17]. Despite some deformation and high forces for two of the four adhesives, rope cutting is a promising separation method for some of the adhesives studied. The following chapter deals with the industrialisation of the rope cutting process using adhesive tape as an example.

Table 3
Results of the analysis of variance, parameter for lowest median cutting force (+ strong influence, − no influence).

Adhesive	wire geometry	wire temperature	cutting speed
Epoxy (EA9497)	+ (round)	+ (cold)	+ (slow)
Polyurethane (7800 A/CD)	–	–	–
Acryle	–	–	–
Acryle tape	+ (twisted)	+ (hot)	+ (slow)

3.2. Industrial solution for glued cell separator

In the following, an industrial implementation of a rope cutter especially for the separation of glued pouch foils is presented. At the same time, the results of the proof of concept are presented.

3.2.1. Construction

An illustration, including labeling of the individual components, is shown in Fig. 7. The design includes two parallel axes with a carriage to support the horizontal drive and driven wheel. The Axes are both position controlled and synchronized and are used to manipulate the cutting tool, in this case the cutting wire. The Drive and driven wheel have V-grooves to accommodate the loop wire, which is clamped between the two wheels. The drive wheel is movably mounted on a small linear axis and has an additional spring system to ensure a constant minimum wire tension. The drive wheel unit also incorporates a tension release mechanism for changing the loop wire. The loop wire is driven by a drive wheel with a servo motor. The lift table is used for storage and height adjustment of the pouch cells to be separated. Inclined gluing surfaces between two pouch cells can be compensated by a height control using light-section sensors and a dynamic servometer responsible for the height adjustment of the lift table. The cell stack (especially the pouch cells) is clamped by a vacuum clamping system located on the lift table. The cell stack is loaded and unloaded by robots such as 6-axis articulated arm robots or SCARA robots. The lateral stabilisation of the rather unstable cell stack is achieved by means of guided pneumatic cylinders, which are mounted laterally. The robot's suction pad grips and stabilises the top cell. Optional heating of the loop wire is performed locally using a heating pad, while a pyrometer allows non-contact temperatures measurement and control of the wire temperature at defined positions. The loop wire can be cleaned by brushing or by heating the wire.

3.2.2. Process parameters and separation strategy

There are different versions of the tool, the loop wire, on the market. Table 4 summarises the main parameters.

An alternative to the endless loop wire would be the linear wire, which requires special construction of the drive and driven wheel. It should be noted that continuous wire movement is not possible in this case.

The process parameters (1) feed rate, (2) cutting speed and (3) wire temperature can be adjusted on the design shown. By varying the above parameters mentioned above, different cutting strategies can be followed. These are summarised in the Table 5. In addition, the feed can be coupled with the wire position via digital cams. Force-controlled cutting can be realised by means of force sensors (either on the vacuum

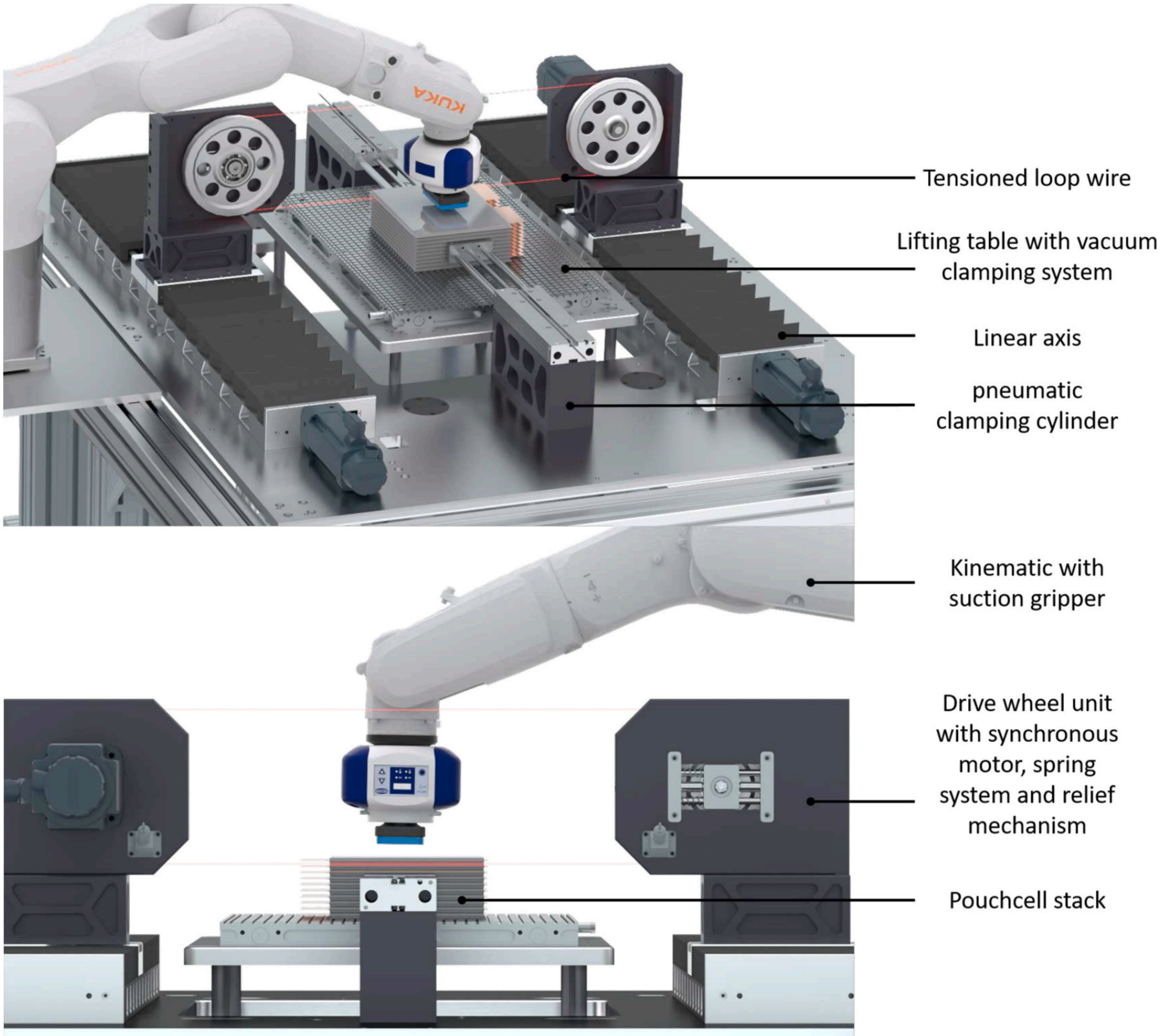

Fig. 7. Conceptional design for industrial glued cell separator. The tensioned loop wire is shown in red.

Table 4
Parameters for the loop rope.

Cross-section geometry	Square	Triangular	Round	Braided
Diameter	0.1	0.15	0.2	...
Material	Iron	Steel	NiCuCr	Nylon
Coating	None	Diamond	...	...

Table 5
Cutting strategy with different process parameters.

Feed rate	Constant	Forward-Back	Shock
Cutting speed	0	Constant	Sine/Zig-Zag
Wire temperature	Room temp.	Near glass transition temp.	...

clamping system, on the slide or on the TCP/suction gripper of the kinematics).

3.2.3. Validation

The previous chapters described the preparation of validation tests to provide a proof of concept for the industrial separator and explained the parameters for the process and the tool. The process is to be validated by finding an appropriate parameter space for the process parameters.

To ensure that all tests are comparable and representative, the tool (wire loop) is referenced prior to each separation test. To achieve this, the wire loop is clamped and moved horizontally against a load cell positioned centrally between the traversing axes (the point of contact of the wire when the cells are separated) by moving the traversing axes. The feed path and the resulting force (load cell) are measured. The angle in the wire loop resulting from the force due to deflection are then calculated. As the wire elongates elastically after a few tests, the wire must be referenced between the tests by increasing the tension. The following values are set for the wire referencing. Feed path: 20 mm; Force (load cell): 15 N. The characteristics of the wire used are shown in the Fig. 8.

In order to identify the process parameter space for a stable cutting process, several cutting tests are carried out with varying feed and cutting speed parameters. Unheated diamond wire is used for the validation tests. The wire was previously referenced (see characteristics). To determine the cutting force, the angle resulting from the deflection of the wire during the cutting process between the wire and the normal between the traversing axes was recorded by camera for each cutting test. The angle was determined using a proprietary image analysis algorithm. The characteristic curve in Fig. 8 allows the resulting force to be deduced from the angle and was thus measured indirectly.

The parameters feed (2;3;5 mm/s) and cutting speed (10.000;30.000;60.000 mm/min) were varied to determine the stable process parameter space. A cutting speed of 30.000 mm/min corresponds to a revolution speed of 54,6 rpm.

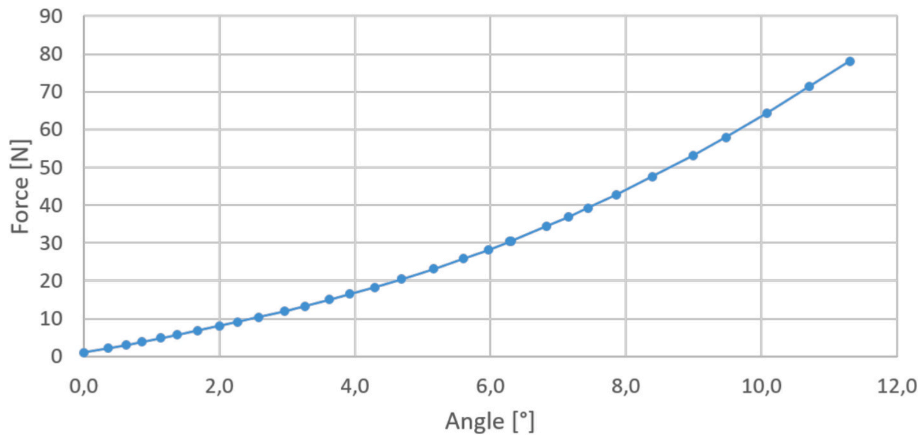

Fig. 8. Characteristic curve of the loop diamond wire.

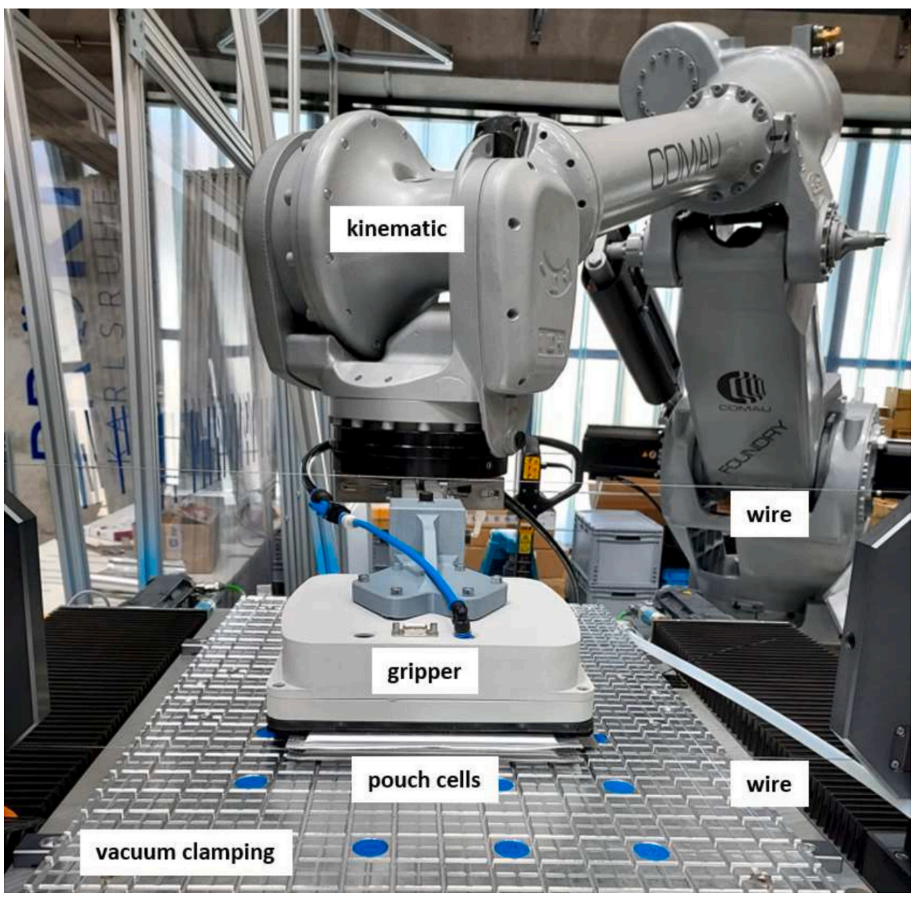

Fig. 9. Real picture of the industrial separator system.

A real image of the industrial separator system is shown in Fig. 9. A total of 25 separation tests were analysed to explore the parameter space. In each test, two glued pouch cells were first clamped on the vacuum clamping system. Then a kinematic (in this case a 6-axis articulated robot from COMAU) grips the upper pouch cell with a suction gripper and lifts it minimally to expand the gap between the two cells. The lift table is then moved to the height of the gap between the two cells. After setting the respective values for feed and cutting speed, the adhesion is separated by a horizontal movement of the traversing axes and a continuous cutting movement of the wire.

The stable parameter space for this process is shown in Fig. 11. The following results were obtained from the tests:

- The selected parameter values result in process forces between approx. 10-30 N
- The force increases with increasing feed rate
- The force decreases with increasing cutting speed

An insufficient feed rate (1 mm/s) combined with a high cutting speed (60.000 mm/min) leads to longer process times. This also results in a longer intervention time from the wire to the cell. With locally small gap sizes and possible wrinkles in the pouch film, the risk of damage and incisions in the cells increases (see incision in Fig. 10a). The tightness of the cells must be maintained for safety reasons. On the other hand, if the feed rate is too high (5 mm/s) and the cutting speed too low (10,000

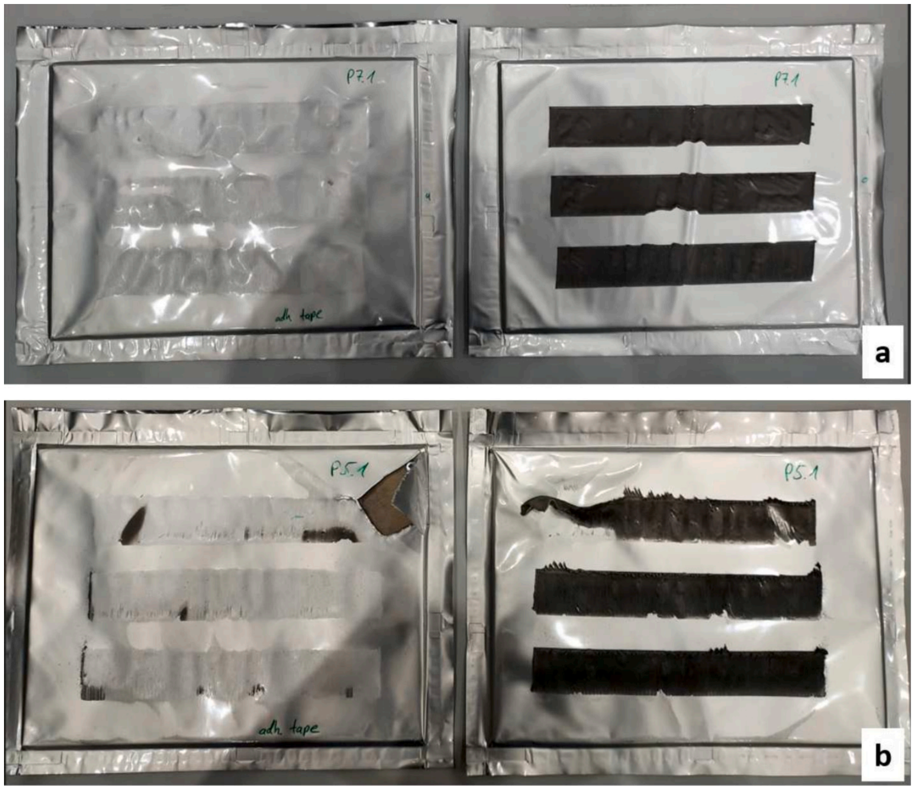

Fig. 10. Fracture patterns of pouch cells glued with adhesive tape (3 M GPH-060GF) after the separation process with stable (a - almost complete adhesion fracture) and unstable (b - mixed fracture, incision in pouch foil) process parameter values.

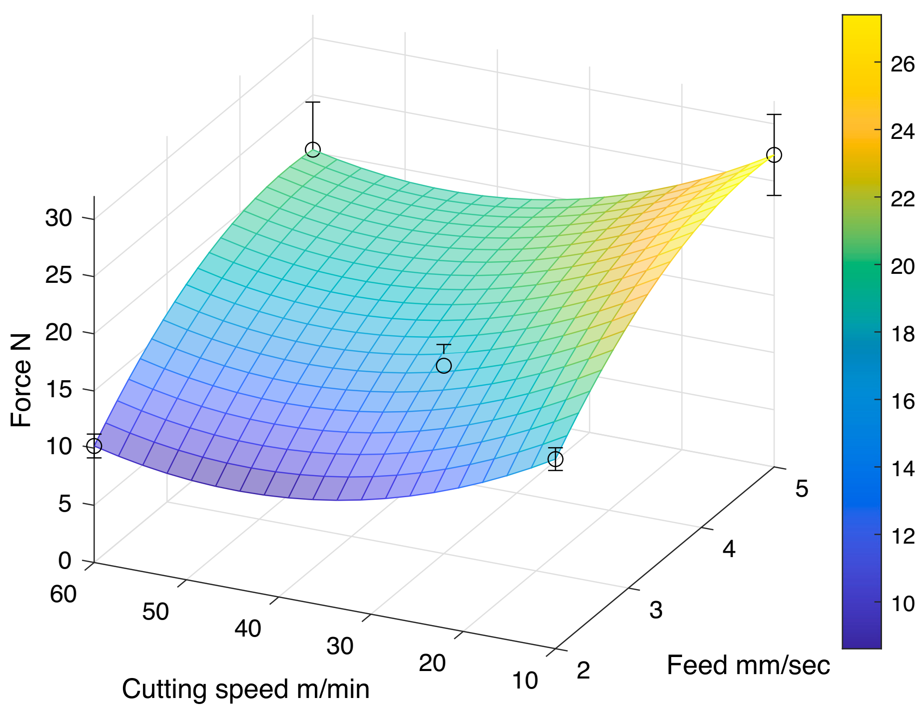

Fig. 11. Forces for different feed and cutting speed.

mm/min), the process forces will increase. This increases the deflection of the wire and the probability of wire breakage increases. These parameter settings results in low process stability.

As can be seen in Fig. 10, all test runs result in almost complete adhesive fractures (predominantly on one joining part, Fig. 10a) or mixed fractures with predominantly adhesive fractures and only minor cohesive fractures (Fig. 10b). One of the two cells usually has almost no adhesive residue after the separation process. Small scratches are then visible on this cell. These are caused by the diamond-studded wire. However, as the scratches do not lead to leakage, the process can be considered stable.

Table 6
Failure patterns during separation process.

Failure patterns / anomalies	Cause	Measures
Delamination	Rough tool surface and localised excessive application of force	Use of flatter tool and process parameter with lower force
Plastic deformation	Localised excessive application of force	process parameter with lower force
Surface scratches	Rough tool surface	Use of flatter tool
Waves	Slip-stick effects	Increasing wire tension
Surface crack	Wire guide and rough tool surface and localised excessive application of force	Check wire guide or control loop insertion

Several failure patterns have been identified in the test series. These failure patterns are listed in Table 6. In addition, causes were identified and possible countermeasures were developed. An increased safety risk is likely to occur only in the case of a surface crack, which must be avoided during the separation process. These only occurred outside the stable process parameter space. Other tool failures included wire cracks (when the critical deflection angle is exceeded), wire abrasion or elongation and adhesive residue on the wire.

In addition, the following process challenges were identified during validation tests:

- Positioning in Z direction and fitting the leading edge
- Limp cell edges could be bent
- Detaching the wire from guide wheels (construction-related)
- *Re*-gluing of the cells

Industrialisation of the process will require further investigation beyond the scope of this work. In particular, these include post-treatments such as the removal of adhesive residues on the separating tool or electrochemical impedance spectroscopy for the electrical characterisation of the cells.

3.3. Conclusion

The separation tests demonstrated an effective separation process using wire. A stable process parameter space was identified in which there is no safety-critical damage to the cells. The cutting process is assisted by the sawing motion of the rotating wire. This can reduce the force required. However, this increases the likelihood of defects such as scratches or cuts.

Validation tests with the industrial prototype machine have demonstrated process stability and safe disassembly of battery cell stacks. In addition to simplifying recycling through mechanical pre-dissection, this also enables other circular economy strategies such as remanufacturing or reuse of the battery cells in a second-life approach.

CRediT authorship contribution statement

Dominik Goes: Writing – original draft. **Eduard Gerlitz:** Writing – review & editing. **Matthias Kagon:** Writing – review & editing. **Hendrik Möllers:** Writing – review & editing. **Florian Kößler:** Writing – review & editing. **Jürgen Fleischer:** Supervision.

Declaration of competing interest

The authors declare that they have no known competing financial interests or personal relationships that could have appeared to influence the work reported in this paper.

Acknowledgments

The authors acknowledge the financial support from the German Ministry for the Environment, Climate and Energy Sector Baden-Württemberg within the DeMoBat project under grant number L7520103.

Data availability

Data will be made available on request.

References

[1] Loctite® aa h8000™: Known as loctite h8000: Technical Data Sheet, 2015.
[2] Battery Thermal Management - Cooltherm Materials: Thermal Management Materials for Electric Vehicle (ev) & Energy Storage Batteries, 2018.
[3] Battery Cell Bonding Applications, 2020.
[4] Thermal Interface Materials for ev Batteries. Low-Density, Low-Abrasive, Silicone-Free, 2020.
[5] L. Aiello, I. Hanzu, G. Gstrein, E. Ewert, C. Ellersdorfer, W. Sinz, Analysis and investigation of thermal runaway propagation for a mechanically constrained lithium-ion pouch cell module, Batteries 7 (2021) 3.
[6] A. Concord, Debonding Technologies for Adhesive Bonded Structures, Dissertation, Brandenburgischen Technischen Universität Cottbus, Cottbus, 2012.
[7] J. Diekmann, C. Hanisch, L. Froböse, G. Schälicke, T. Loellhoeffel, A.-S. Fölster, A. Kwade, Ecological recycling of lithium-ion batteries from electric vehicles with focus on mechanical processes, J. Electrochem. Soc. 164 (1) (2017) A6184–A6191.
[8] DIN Deutsches Institut für Normung e.V, Konstruktionsklebstoffe - leitlinie zum trennen und rückgewinnen von klebstoffen und fügeteilen aus geklebten verbindungen, Dezember, 2020.
[9] DIN Deutsches Institut für Normung e.V, Klebstoffe- t-schälprüfung für geklebte verbindungen aus flexiblen fügeteilen, Mai, 2022.
[10] DIN Deutsches Institut für Normung e.V, Lithium-ionen-sekundärzellen für den antrieb von elektrostraßenfahrzeugen, 2017.
[11] DIN Deutsches Institut für Normung e.V, Klebstoffe – bestimmung der zugscherfestigkeit von Uberlappungsklebungen; deutsche fassung en 1465:2009, Juli, 2009.
[12] DIN Deutsches Institut für Normung e.V, Fertigungsverfahren fügen: Teil 8, Kleben, September 2003.
[13] DIN Deutsches Institut für Normung e.V, Fertigungsverfahren zerlegen: Einordnung, unterteilung, begriffe, September 2003.
[14] T. Elwert, F. Römer, K. Schneider, Q. Hua, M. Buchert, Recycling of Batteries from Electric Vehicles, Springer International Publishing, Cham, 2018, pp. 289–321.
[15] Für Strassen-und Verkehrswesen e.V., F, Merkblatt über die statistische Auswertung von Prüfergebnissen, ausg 2003rd, vol. 2, Erkennen und Behandeln von Ausreißern of FGSV, Köln, 2003, 926,2.
[16] L. Gaines, The future of automotive lithium-ion battery recycling: charting a sustainable course, Sustain. Mater. Technol. 1-2 (2014) 2–7.
[17] E. Gerlitz, M. Greifenstein, J.-P. Kaiser, D. Mayer, G. Lanza, J. Fleischer, Systematic identification of hazardous states and approach for condition monitoring in the context of li-ion battery disassembly, in: *Procedia CIRP 107* (2022), 308–313. Leading Manufacturing Systems Transformation – Proceedings of the 55th CIRP Conference on Manufacturing Systems, 2022.
[18] S.V. Gopinadh, V. Anoopkumar, M.J.N. Ansari, D. Srivastava, M.A. Raj, B. John, A. Samridh, P.S. Vijayakumar, T.D. Mercy, Lithium-ion pouch cells: An overview, in: M.K. Jayaraj, A. Antony, P.P. Subha (Eds.), Energy harvesting and storage: Fundamentals and materials, Springer Nature Singapore, 2024, pp. 209–224.
[19] G. Habenicht, Kleben: Grundlagen, Technologien, *Anwendungen*, Springer, Berlin Heidelberg, Berlin, Heidelberg, 2009.
[20] G. Habenicht, Kleben - erfolgreich und fehlerfrei, Springer Fachmedien Wiesbaden, Wiesbaden, 2016.
[21] G. Harper, R. Sommerville, E. Kendrick, L. Driscoll, P. Slater, R. Stolkin, A. Walton, P. Christensen, O. Heidrich, S. Lambert, A. Abbott, K. Ryder, L. Gaines, P. Anderson, Recycling lithium-ion batteries from electric vehicles, Nature 575 (7781) (2019) 75–86.
[22] J. Kelly, See a 2011 Nissan Leaf Battery Dissected Professionally: Video, 2024.
[23] M.M. Keshavarzi, M. Gilaki, E. Sahraei, Characterization of in-situ material properties of pouch lithium-ion batteries in tension from three-point bending tests, Int. J. Mech. Sci. 219 (2022) 107090.
[24] G. Kovachev, H. Schröttner, G. Gstrein, L. Aiello, I. Hanzu, H.R.M. Wilkening, A. Foitzik, M. Wellm, W. Sinz, C. Ellersdorfer, Analytical dissection of an automotive li-ion pouch cell, Batteries 5 (2019) 4.
[25] A. Kwade, J. Diekmann, Recycling of Lithium-Ion Batteries, Springer International Publishing, Cham, 2018.
[26] C. Lammel, P. Schaumeier, Trennen struktureller klebverbindungen in sekundenbruchteilen. *adhäsion*, Kleben Dichten *53* (11) (2009) 28–31.
[27] L. Li, P. Zheng, T. Yang, R. Sturges, M.W. Ellis, Z. Li, Disassembly automation for recycling end-of-life lithium-ion pouch cells, JOM 71 (12) (2019) 4457–4464.
[28] A. Maurer, J. Kalka, A. Wiessler, Smart design of electric vehicle batteries and power electronics using thermal interface materials, in: Proceedings of the EVS30 International Electric Vehicle Symposium, Germany, Stuttgart, 2017, pp. 9–11.

[29] G.W. Mueller, T. Kick, BASIC-Programme für die angewandte Statistik: 32 Programme für Kleincomputer, 2., verb. u. erw. aufl. ed, Oldenbourg, München, 1985.
[30] M. Pomykala, Electric vehicles and the growing significance of adhesives and sealants for battery assembly 9 (2020) 3.
[31] Y. Qu, B. Xing, C. Wang, Y. Xia, Simplified layered model of pouch cell for varied load cases: an indentation and three-point bending study, J. Energy Storag. 59 (2023) 106476.
[32] M. Rasche, Handbuch Klebetechnik, Carl Hanser Verlag, 2012.
[33] S. Sims, V. Gettwert, H. Urban, et al., Energetic materials. synthesis, characterization, processing, in: International Annual Conference #47, Fraunhofer-Institut für Chemische Technologie, 2016, p. 9.
[34] M. Zhou, B. Li, J. Li, Z. Xu, Pyrometallurgical technology in the recycling of a spent lithium ion battery: evolution and the challenge, ACS ES&T Eng. 1 (10) (2021) 1369–1382.